ORCA – Online Research @ Cardiff

This is an Open Access document downloaded from ORCA, Cardiff University's institutional repository:https://orca.cardiff.ac.uk/id/eprint/102140/

This is the author’s version of a work that was submitted to / accepted for publication.

Citation for final published version:

Delmonte, V., Specht, J. F., Jakubczyk, T., Hofling, S., Kamp, M., Schneider, C., Langbein, Wolfgang Werner , Nogues, G., Richter, M. and Kasprzak, J. 2017. Coherent coupling of individual quantum dots measured with phase-referenced two-dimensional spectroscopy: photon echo versus double quantum coherence. Physical Review B 96 , 041124(R). 10.1103/PhysRevB.96.041124

Publishers page: https://doi.org/10.1103/PhysRevB.96.041124

Please note:
Changes made as a result of publishing processes such as copy-editing, formatting and page numbers may not be reflected in this version. For the definitive version of this publication, please refer to the published source. You are advised to consult the publisher’s version if you wish to cite this paper.

This version is being made available in accordance with publisher policies. See http://orca.cf.ac.uk/policies.html for usage policies. Copyright and moral rights for publications made available in ORCA are retained by the copyright holders.

Coherent coupling of individual quantum dots measured with phase-referenced two-dimensional spectroscopy: photon echo versus double quantum coherence

Valentin Delmonte,[1, 2] Judith F. Specht,[3] Tomasz Jakubczyk,[1, 2] Sven Höfling,[4, 5] Martin Kamp,[4]
Christian Schneider,[4] Wolfgang Langbein,[6] Gilles Nogues,[1, 2] Marten Richter,[3] and Jacek Kasprzak[1, 2, *]
[1] *Univ. Grenoble Alpes, F-38000 Grenoble, France*
[2] *CNRS, Institut Néel, "Nanophysique et semiconducteurs" group, F-38000 Grenoble, France*
[3] *Institut für Theoretische Physik, Nichtlineare Optik und Quantenelektronik,*
Technische Universität Berlin, Hardenbergstrasse 36, 10623 Berlin, Germany
[4] *Technische Physik, University of Würzburg, Würzburg, Germany*
[5] *SUPA, School of Physics and Astronomy, University of St Andrews, St Andrews, KY16 9SS, United Kingdom*
[6] *School of Physics and Astronomy, Cardiff University,*
The Parade, Cardiff CF24 3AA, United Kingdom

We employ two-dimensional (2D) coherent, nonlinear spectroscopy to investigate couplings within individual InAs quantum dots (QD) and QD molecules. Swapping pulse ordering in a two-beam sequence permits to distinguish between rephasing and non-rephasing four-wave mixing (FWM) configurations. We emphasize the non-rephasing case, allowing to monitor two-photon coherence dynamics. Respective Fourier transform yields a double quantum 2D FWM map, which is corroborated with its single quantum counterpart, originating from the rephasing sequence. We introduce referencing of the FWM phase with the one carried by the driving pulses, overcoming the necessity of its active-stabilization, as required in 2D spectroscopy. Combining single and double quantum 2D FWM, provides a pertinent tool in detecting and ascertaining coherent coupling mechanisms between individual quantum systems, as exemplified experimentally.

Nuclear magnetic resonance (NMR) spectroscopy conceived phase-locked, multi-pulse techniques, yielding multi-dimensional spectra by Fourier transforming temporal sequences into respective frequency coordinates [1, 2]. The possibility to spread the response of biological or chemical molecules of high structural complexity, especially proteins, across many axes enabled to assess their spatial form and to understand inter-atomic interactions and couplings. The idea to selectively address and evolve subsets of transitions from congested spectra via multi-pulse toolbox, and then projecting the results onto two-dimensional (2D) or three-dimensional diagrams, is a far-reaching legacy of NMR. At a juncture of coherent spectroscopy and condensed matter physics, 2D spectroscopy provided insight into dynamics and couplings of many-body optical excitations in solids, in particular of excitons in semiconductor quantum wells [3–5] and novel 2D layered materials [6], as well as in ensembles of quantum dots [7, 8] (QDs) or nanocrystals [9]. A principal tool in these investigations is k-resolved four-wave mixing (FWM) spectroscopy and its extensions probing multi-wave mixing processes [4].

FWM spectroscopy has been exploited over the years to study Coulomb interactions and related ultrafast coherent dynamics of excitons in semiconductors [10–14]. In these ensemble experiments, a strong inhomogeneous broadening usually is an obstacle to implement coherent control protocols. This issue is largely overcome, when restricting the study to individual excitons. Moreover, in en exciting context of optical information processing in solids, establishing controlled channels of coupling within a set of few-level systems, represents a truly challenging goal. For these reasons, it its necessary to access coherence of individual excitons, and then to ascertain mechanism of their coherent interactions, involving both Coulomb (local) and radiation (long-range) mediated phenomena. The present work represents a step forward in this field.

FWM microscopy of single QD excitons [15] was previously accomplished by phase-sensitive optical heterodyning combined with interferometric detection, efficiently subtracting resonant background and permitting colinear geometry of the excitation pulses. Recently, detection sensitivity of intrinsically weak single QD FWM has been enhanced substantially by using photonic nanostructures, improving the QD coupling with external laser beams [16–18]. Here, we perform FWM spectroscopy of individual InAs QDs embedded in a low-Q semiconductor microcavity [19]. We point out two advancements with respect to our recent reports [16, 20]: Firstly, we demonstrate 2D FWM constructed from two-photon coherences — known as double quantum 2D FWM [21–24] — driven on individual transitions, specifically QD exciton-biexciton systems (GXB) [25]. Secondly, we introduce referencing of the FWM phase, offering convenient alternative for its active-stabilization, which is widely believed to be required in 2D spectroscopy. Using the one-quantum and two-quantum spectroscopy, we have measured single QDs and a QD molecule. A comparison of the spectra signatures to theory allowed us to identify the nature of the internal coupling mechanism in the QD molecule system. Our work shows that the combined single and double quantum 2D spectroscopy is a powerful tool to reveal and understand coherent cou-

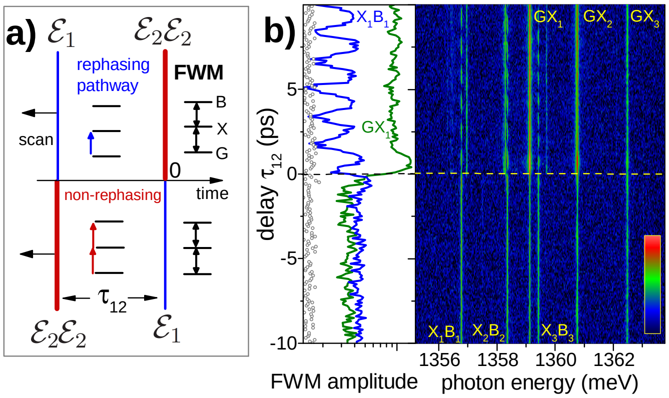

FIG. 1. **Rephasing and non-rephasing pathways in two-beam four-wave mixing of individual quantum dots.** (a) Two possible pulse sequences in, so-called, positive (negative) delays τ_{12}, corresponding to the rephasing (non-rephasing) FWM pathways. The non-rephasing pathway involves a two-photon coherence between the ground state (G) and a two-particle state, here a quantum dot biexciton (B). (b) Measured FWM amplitude as a function of τ_{12} on a few InAs QDs embedded in a low-Q microcavity. Impinging $\mathcal{E}_1$, $\mathcal{E}_2$ intensities of (150, 600) nW correspond to pulse areas of around (0.4π, 0.8π), significantly beyond the $\chi^{(3)}$ limit, generating a pronounced exciton-biexciton beating.

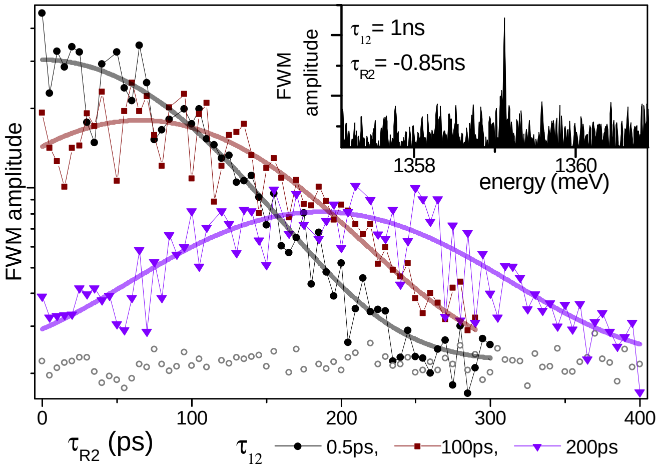

FIG. 2. **Photon-echo formation on a single QD exciton measured upon FWM rephasing pathway**. The delay τ_{R2}, between the reference $\mathcal{E}_\mathrm{R}$ and $\mathcal{E}_2$, is scanned for different values of τ_{12}, as indicated. Formation of the photon echo is observed: a Gaussian form of the FWM transient is fully recovered for $\tau_{12} > \hbar/\sigma$. Temporal width of the echo yields the inhomogeneous broadening σ. Inset: By adjusting τ_{R2}, one shifts the temporal detection window towards the echo, such that the FWM signal can be retrieved via spectral interference even for delays exceeding temporal resolution of the setup, defined by the spectrometer. This is here exemplified for $\tau_{12} = 1\,\mathrm{ns}$ and $\tau_{R2} = -0.85\,\mathrm{ns}$.

pling and excitation transfer mechanisms - an interdisciplinary issue spanning from biology and photo-chemistry, to quantum engineering. The results are especially pertinent for the latter area, as we open new avenues of research in quantum control of optically active nanoscopic two-level and few-level systems in solids.

To acquire the FWM spectra [16], we use a pair of 100 fs laser pulses: $\mathcal{E}_1$ and $\mathcal{E}_2$, with a variable delay τ_{12}, positive for $\mathcal{E}_1$ leading. They are frequency shifted by $\Omega_1 = 80\,\mathrm{MHz}$ and $\Omega_2 = 80.77\,\mathrm{MHz}$, respectively, using acousto-optic deflectors. FWM heterodyne beat with a reference field $\mathcal{E}_\mathrm{R}$ is retrieved at $2\Omega_2 - \Omega_1 = 81.54\,\mathrm{MHz}$ frequency, carrying the lowest order response $\mathcal{E}_1^\star\mathcal{E}_2\mathcal{E}_2$ (where $\star$ denotes complex conjugate) and also higher orders with the same phase evolution. The signal is spectrally dispersed using a spectrometer, detected with a CCD camera and retrieved in amplitude and phase by applying spectral interferometry. $\mathcal{E}_\mathrm{R}$ arrives a few picoseconds prior to $\mathcal{E}_2$, unless specified otherwise.

As shown in Fig. 1 a, in two-beam FWM, the first pulse $\mathcal{E}_1$ induces coherence, which evolves during τ_{12}, to be then converted into FWM by the second pulse $\mathcal{E}_2$. The lowest electronic excitations of a neutral QD can be cast into three categories of states: a ground state (G), single excitons (X) and two-exciton states, known as biexcitons (B). GX transitions are addressed by one-photon coherence driven by $\mathcal{E}_1$, which is converted to FWM of GX and XB by a density grating $\mathcal{E}_1^\star\mathcal{E}_2$ on G and X [20, 26]. Inverting temporal ordering of the two light pulses, GB transition can be inspected by a two-photon coherence induced by $\mathcal{E}_2$, transformed into FWM of both transitions at the arrival of $\mathcal{E}_1$ [20, 26]. The simple three-level system of Fig. 1 a illustrates the case of a neutral QD driven along one of its polarization axes. For a single two-level system, like a QD trion, FWM can be only created for $\tau_{12} > 0$ from one-photon coherence induced by $\mathcal{E}_1$, since the trion system cannot be doubly excited within the employed spectral bandwidth. In fact, two transitions in Fig. 1 b show strictly no signal for $\tau_{12} < 0$ and are attributed to trion transitions. Therein, we also recognize pairs of exciton-biexcitons, labeled as: $GX_1 - X_1B_1$, $GX_2 - X_2B_2$, $GX_3 - X_3B_3$ occurring in three distinct QDs. FWM exhibits a pronounced beating as a function of $\tau_{12} > 0$, with a period corresponding to B binding energy, which is induced beyond $\chi^{(3)}$ regime by high order contributions propagating at the FWM frequency [20, 27]. Instead, for $\tau_{12} < 0$ FWM is equally created on GX and XB transitions, with no beating.

Time-resolved FWM transient created upon the two pulse configurations displays different characteristics. For $\tau_{12} > 0$, there is a phase-conjugation between $\mathcal{E}_1$ and FWM. Owing to the rephasing, FWM of an inhomogeneously broadened system has a Gaussian form, with a maximum at $t = \tau_{12}$ and temporal width inversely proportional to the probed spectral inhomogeneous broadening σ. Importantly, time-integrated amplitude of such photon echo is not sensitive on σ, instead the homogeneous broadening is probed through the τ_{12}-dependence.

At a level of individual transitions, σ is accumulated due to a residual spectral wandering in time-averaged measurement [17, 18, 26, 28]. For σ in μeV range, which is a case even for high quality QD systems, the echo width becomes comparable or larger than the temporal sensitivity, given by the spectrometer resolution (here about 120 ps). To demonstrate formation of such a broad echo [18], we scan the delay τ_{R2}, between $\mathcal{E}_{\rm R}$ and $\mathcal{E}_2$, for three different τ_{12}, as shown in Fig. 2. The echo develops fully only for $\tau_{12} = 200\,$ps, from its width (FWHM) $t_\sigma = \hbar/\sigma = (214 \pm 33)\,$ps we retrieve spectral inhomogeneous broadening $8\ln(2)\sigma = 8\ln(2)\hbar/t_\sigma = (17 \pm 3)\,\mu$eV (FWHM). By advancing τ_{R2} sufficiently close to the maximum of the echo, the temporal detection window is brought toward its maximum, permitting to retrieve FWM spectral interference for delays significantly exceeding the temporal sensitivity of the spectrometer, as shown in the inset for $\tau_{12} = 1\,$ns and $\tau_{R2} = -0.85\,$ns.

For $\tau_{12} < 0$ there is no strict phase conjugation between two-photon coherence and FWM, and therefore the photon echo is absent. In Fig. 3 (a, b) we show (t, τ_{12})-resolved maps of the FWM amplitude measured on GX_1 and X_1B_1 transitions, respectively. As τ_{12} is increased towards more negative values, FWM decay becomes more pronounced, owing to a non-rephasing character of the signal. The two-photon coherence dynamics of GX_1 and X_1B_1, i.e. respective time-integrated FWM versus τ_{12}, are presented in Fig. 3 a and b. From the exponential decay of $\rm GX_1$ and $\rm X_1B_1$ we retrieve two-photon (biexciton) dephasing [29, 30] $T_{TP}(GX_1, X_1B_1) = (75 \pm 3, 65 \pm 3)\,$ps. Similar values of T_{TP} are obtained by analyzing two other GX-XB pairs. Note that, in homogenously broadened GXB system, T_{TP} should be the same when inferring it either from GX or XB transition. A slightly faster biexciton dephasing evaluated from the X_1B_1 decay, is attributed to its stronger inhomogeneous broadening via spectral wandering with respect to $\mathrm{G}X_1$: the latter is due to energy fluctuations of the exciton level only, whereas the former is sensitive on wandering of both exciton and biexciton levels [31, 32]. These spectral fluctuations do not have to be correlated, and thus yield a shorter T_{TP} when reading it out from $\rm X_1B_1$.

To illustrate couplings in the probed system of a few QDs, we Fourier-transform FWM(ω_3, τ_{12}) sequences with respect to the delay τ_{12}. The experimental setup is encapsulated, providing a passive stabilization of the phase during the acquisition. However, the phase relationship between FWM measured for subsequent τ_{12} is inevitably lost and can only be achieved via active-stabilization [33, 34], which is not implemented here. The knowledge of the FWM phase for subsequent delays τ_{12} is a precondition to execute the Fourier transform yielding 2D FWM. In our previous works [20, 35], we have circumvent this issue by imposing a phase relationship onto the data by choosing a separated transition in the spectral domain, acting as a local oscillator, and setting its phase to zero for all delays. We then applied this phase factor globally to the full spectrum, adjusting all other frequencies versus τ_{12}, accordingly. Such transformation remains justified, as long as the guiding transition to correct for, in particular exhibiting no coherent coupling, is available in the spectrum. This generally is not the case. To overcome this experimental limitation, we have conceived a post-treatment protocol permitting to reference the FWM phase, using auxiliary spectral interferences of $\mathcal{E}_{\rm R}$ with the driving pulses [36].

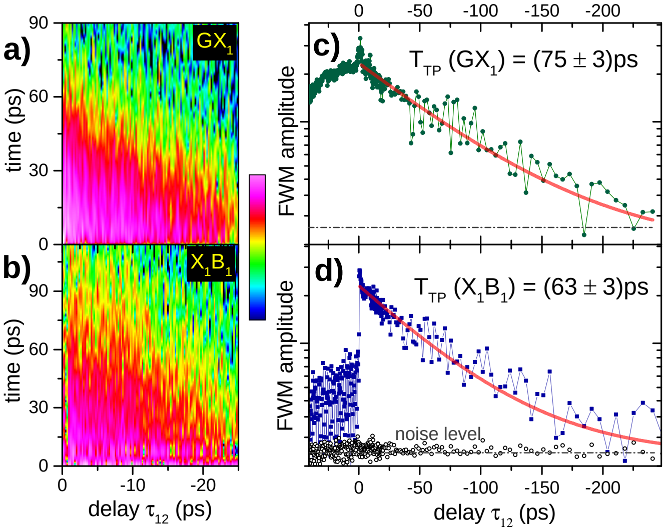

FIG. 3. **Coherent dynamics of an exciton-biexciton system measured at the non-rephasing FWM configuration,** $\tau_{12} < 0$ (a, b) Time-resolved FWM transient measured at $\rm GX_1$ and $\rm X_1B_1$ for negative delays. Due to the non-rephasing configuration, the FWM decay becomes more pronounced when increasing delay. (c, d) Two-photon coherence dynamics, induced between G and B (also known as a biexciton coherence), measured at the non-rephasing FWM configuration. The two-photon dephasing time is retrieved from the exponential decay of $\rm GX_1$ and $\rm X_1B_1$ transitions.

In Fig. 4 we present 2D FWM obtained from the set of QDs highlighted in Fig. 1. For $\tau_{12} > 0$, FWM generated by all resonances driven by $\mathcal{E}_1$, forms a diagonal in the resulting 2D spectrum. This includes, single trions and neutral excitons, but also biexcitons - the latter can directly be driven by $\mathcal{E}_1$ beyond the $\chi^{(3)}$ limit [20], as applied here [37]. The biexcitons are off-diagonally shifted by their respective binding energies of a few meV, and form square-like features in 2D FWM under strong excitation, i.e. close to ($\pi/2$, π) area of ($\mathcal{E}_1$, $\mathcal{E}_2$) pulses. 2D FWM resulting from $\tau_{12} < 0$ is shown in Fig. 4 b. FWM originates from a corresponding two-photon resonance driven by $\mathcal{E}_2$. Here, the two-photon energy corresponds to the sum GX and XB transition energies. In such non-rephasing 2D FWM, we retrieve the response of GXB systems, whereas exciton complexes without doubly excited states within the excitation bandwidth, such

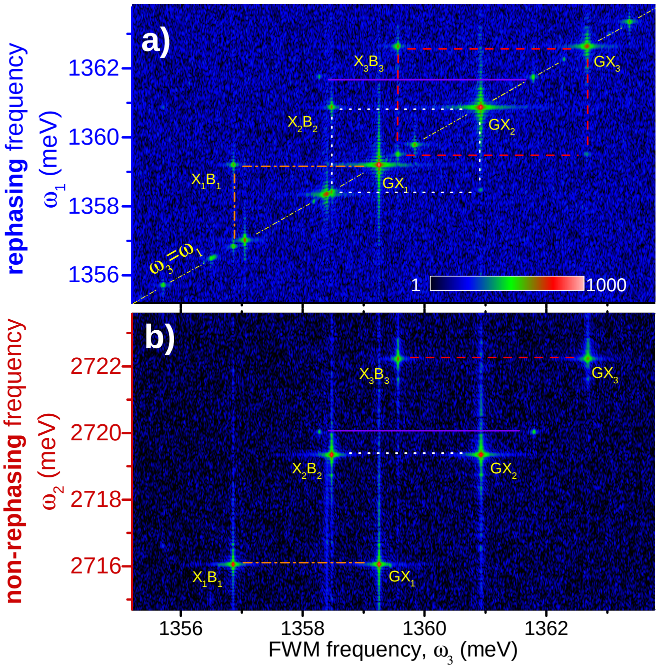

FIG. 4. **Two-dimensional FWM spectroscopy of exciton complexes in a few InAs QDs probed along the rephasing (a) and non-rephasing (b) pathways.** Four exciton-biexciton systems in different QDs are indicated dash-dotted, dotted, dashed and solid lines, respectively.

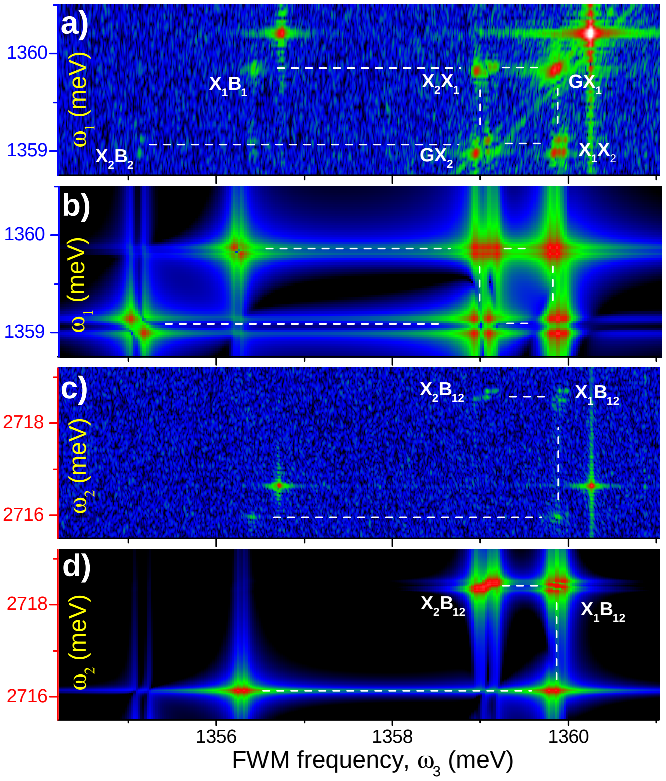

FIG. 5. **Quantum dot molecule, consisting of two electrostatically coupled InAs QDs, observed in single and double quantum 2D FWM.** Measured rephasing (a) and non-rephasing (c) 2D FWM spectra revealing coherent couplings between two QDs. Corresponding simulations [44] are shown in (b) and (d). The signatures belonging to this QD molecule are marked by dashed lines. An additional exciton-biexciton pair in (a) and (c) at (1360.3, 1356.8) meV occurs in other QD, not involved in the molecule formation, thus not included in the calculated spectra.

as singly charged QDs, do not contribute.

Fig. 5 a and c show the measured rephasing and non-rephasing 2D spectra recorded at another position at the sample. In the following, we focus on the two QDs that show up as transitions GX_1 and GX_2 on the diagonal of the rephasing spectrum with resonance energies E_1=1359.7 meV and E_2=1358.95 meV - via hyperspectral imaging these are found to be within 0.5 μm vicinity [35, 38]. The peak pattern highlighted by the dashed lines differs from the signatures observed in Fig. 4 in two major respects: First, spin-orbit coupling of the two circularly polarized excitons within each QD leads to linearly polarized exciton eigenstates, where each QD is described by a four-level system [20]. This causes a splitting of each exciton resonance on the diagonal of the rephasing spectrum into clusters of four peaks, observed in Fig. 5 a and c. Second, besides the X_1B_1 and X_2B_2 peaks that are redshifted along the FWM axis by the intradot biexciton binding energies Δ_1=-3.3 meV and Δ_2=-3.6 meV, respectively, we observe two off-diagonal cross peaks labeled X_2X_1 and X_1X_2 at the spectral positions ($\omega_3 = E_2; \omega_1 = E_1$) (upper cross peak) and ($\omega_3 = E_1; \omega_1 = E_2$) (lower cross peak). The appearance of these cross peaks clearly indicates a coherent interdot coupling between the two QDs: The electrostatic Coulomb coupling leads to an energy renormalization of the interdot biexciton B_{12} consisting of one exciton in each QD. The biexciton shift lifts the symmetry of the lower GX_1 (GX_2) and higher X_1B_{12} (X_2B_{12}) transitions, such that the quantum pathways involving these transitions do not destructively interfere anymore and cross peaks show up [35, 39]. The electrostatic interaction Δ_{12} between two excitons located in two different QDs is small compared to the intradot biexciton binding energies Δ_1 and Δ_2. In fact, spectrally-resolved FWM amplitude [40] reveals that it is only of the order of $\Delta_{12} = 90\,\mu$eV and it shifts the interdot biexciton towards higher energies, showing up as blueshifted [41] high-energy shoulders of the exciton resonance peaks. This interpretation is supported by calculations [42, 43] of the rephasing and non-rephasing 2D signals depicted in Fig. 5 b and d.

In the non-rephasing two-quantum spectrum, the coupling of the two QDs manifests itself in a peak pair labeled X_1B_{12} and X_2B_{12} at the interaction-shifted two-exciton transition GB_{12} (energy $\omega_2 = E_1 +$

$E_2 + \Delta_{12}$ =2718.74 meV) with FWM frequencies $\omega_3 = E_1$ =1359.7 meV and $\omega_3 = E_2$ =1358.95 meV, respectively. Theoretical calculations [43] also suggest that exciton transfer processes between the two QDs such as dipole-induced (Förster) interaction and Dexter-type coupling via wave-function overlap are negligible [45]: First, these coupling types are expected to be in the μeV range [35] and therefore difficult to detect considering our spectrometer resolution of 25 μeV. Second, they would lead to additional peaks for an intradot biexciton in one QD after the first pulse has created a single-exciton in the other QD. These peaks are not observed in the spectra indicating that exciton transfer elements are negligible [46].

An interesting feature about the observed QD molecule is that, in contrast to the other isolated exciton-biexciton systems, the two coupled QDs show a pronounced fine-structure splitting (FSS) of the order of 60 μeV and 140 μeV, respectively. This is around 5 times higher than the FSS typically present in these QDs [20]. Moreover, the FSS of the other isolated exciton-biexciton systems in our sample (see also Fig. 4) is not visible since the direction of the linear excitation/reference polarization was chosen to be parallel to the anisotropy axis. The observation of such a pronounced FSS only for the resonances associated with the QD molecule therefore suggests that the spatial proximity of the two coupled QDs altered the local symmetry of the confinement, changing the magnitude of the FSS and the polarization of the excitonic transitions.

In summary, we have implemented phase-referenced double quantum 2D FWM spectroscopy of individual quantum systems. By merging it with the single quantum counterpart, we have ascertained coherent couplings between excitons the structure of (bi-)exciton states, and coupling energies in single InAs QDs and in a quantum dot molecule. Optical selection rules of the latter were investigated theoretically. This methodology is appealing to infer electronic couplings and charge transfer in deterministically defined QD molecules [47, 48] and propagative coherence in photonic molecules [49]. By merging it with recently developed multi-wave mixing toolbox [16], it could be also used to visualize and control polaritonic couplings in solid state cavity-quantum electrodynamics [50].

Note added: 2D FWM in rephasing and non-rephasing configurations of individual transitions in interface fluctuation QD are also reported in Ref. [51].

ACKNOWLEDGEMENTS

We gratefully acknowledge the financial support by the European Research Council (ERC) Starting Grant PICSEN (grant no. 306387). J.S. and M.R. acknowledge financial support by SFB 787 and GRK 1558.

---

[*] jacek.kasprzak@neel.cnrs.fr

[1] K. Wüthrich, Journal of Biomolecular NMR **27**, 13 (2003).
[2] L. M. K. Vandersypen and I. L. Chuang, Rev. Mod. Phys. **76**, 1037 (2005).
[3] K. W. Stone, K. Gundogdu, D. B. Turner, X. Li, S. T. Cundiff, and K. A. Nelson, Science **324**, 1169 (2009).
[4] D. Turner and K. Nelson, Nature **466**, 1089 (2010).
[5] G. Moody, I. A. Akimov, H. Li, R. Singh, D. R. Yakovlev, G. Karczewski, M. Wiater, T. Wojtowicz, M. Bayer, and S. T. Cundiff, Phys. Rev. Lett. **112**, 097401 (2014).
[6] K. Hao, L. Xu, P. Nagler, A. Singh, K. Tran, C. K. Dass, C. Schüller, T. Korn, X. Li, and G. Moody, Nano Letters **16**, 5109 (2016).
[7] G. Moody, R. Singh, H. Li, I. A. Akimov, M. Bayer, D. Reuter, A. D. Wieck, A. S. Bracker, D. Gammon, and S. T. Cundiff, Phys. Rev. B **87**, 041304 (2013).
[8] G. Moody, R. Singh, H. Li, I. A. Akimov, M. Bayer, D. Reuter, A. D. Wieck, and S. T. Cundiff, Phys. Rev. B **87**, 045313 (2013).
[9] E. Cassette, J. C. Dean, and G. D. Scholes, Small **12**, 2234 (2016).
[10] H. Wang, K. Ferrio, D. G. Steel, Y. Z. Hu, R. Binder, and S. W. Koch, Phys. Rev. Lett. **71**, 1261 (1993).
[11] M. U. Wehner, M. H. Ulm, D. S. Chemla, and M. Wegener, Phys. Rev. Lett. **80**, 1992 (1998).
[12] D. S. Chemla and J. Shah, Nature **411**, 549 (2001).
[13] J. M. Shacklette and S. T. Cundiff, Phys. Rev. B **66**, 045309 (2002).
[14] T. Voss, I. Rückmann, J. Gutowski, V. M. Axt, and T. Kuhn, Phys. Rev. B **73**, 115311 (2006).
[15] W. Langbein and B. Patton, Phys. Rev. Lett. **95**, 017403 (2005).
[16] F. Fras, Q. Mermillod, G. Nogues, C. Hoarau, C. Schneider, M. Kamp, S. Höfing, W. Langbein, and J. Kasprzak, Nat. Phot. **10**, 155 (2016).
[17] Q. Mermillod, T. Jakubczyk, V. Delmonte, A. Delga, E. Peinke, J.-M. Gérard, J. Claudon, and J. Kasprzak, Phys. Rev. Lett. **116**, 163903 (2016).
[18] T. Jakubczyk, V. Delmonte, S. Fischbach, D. Wigger, D. E. Reiter, Q. Mermillod, P. Schnauber, A. Kaganskiy, J.-H. Schulze, A. Strittmatter, S. Rodt, W. Langbein, T. Kuhn, S. Reitzenstein, and J. Kasprzak, ACS Photonics **3**, 2461 (2016).
[19] S. Maier, P. Gold, A. Forchel, N. Gregersen, J. Mørk, S. Höfling, C. Schneider, and M. Kamp, Opt. Express **22**, 8136 (2014).
[20] Q. Mermillod, D. Wigger, V. Delmonte, D. E. Reiter, C. Schneider, M. Kamp, S. Höfling, W. Langbein, T. Kuhn, G. Nogues, and J. Kasprzak, Optica **3**, 377 (2016).
[21] J. Kim, S. Mukamel, and G. D. Scholes, Accounts of Chemical Research **42**, 1375 (2009).
[22] D. Karaiskaj, A. D. Bristow, L. Yang, X. Dai, R. P. Mirin, S. Mukamel, and S. T. Cundiff, Phys. Rev. Lett. **104**, 117401 (2010).
[23] D. B. Turner, P. Wen, D. H. Arias, and K. A. Nelson, Phys. Rev. B **84**, 165321 (2011).
[24] X. Dai, M. Richter, H. Li, A. D. Bristow, C. Falvo, S. Mukamel, and S. T. Cundiff, Phys. Rev. Lett. **108**, 193201 (2012).

[25] B. P. Fingerhut, M. Richter, J.-W. Luo, A. Zunger, and S. Mukamel, Ann. Phys. **525**, 31 (2013).

[26] J. Kasprzak, S. Portolan, A. Rastelli, L. Wang, J. D. Plumhof, O. G. Schmidt, and W. Langbein, New J. Phys. **15**, 055006 (2013).

[27] W. Langbein, T. Meier, S. Koch, and J. Hvam, J. Opt. Soc. Am. B **18**, 1318 (2001).

[28] B. Patton, W. Langbein, U. Woggon, L. Maingault, and H. Mariette, Phys. Rev. B **73**, 235354 (2006).

[29] E. J. Mayer, G. O. Smith, V. Heukenroth, J. Kuhl, K. Bott, A. Schulze, T. Meier, D. Bennhardt, S. W. Koch, and P. Thomas, Phys. Rev. B **50**, 14730 (1994).

[30] H. P. Wagner, W. Langbein, and J. M. Hvam, Phys. Rev. B **59**, 4584 (1999).

[31] W. Langbein and J. M. Hvam, Phys. Rev. B **61**, 1692 (2000).

[32] W. Langbein and J. M. Hvam, phys. stat. sol. (a) **190**, 167 (2002).

[33] A. D. Bristow, D. Karaiskaj, X. Dai, and S. T. Cundiff, Opt. Express **16**, 18017 (2008).

[34] J. Helbing and P. Hamm, J. Opt. Soc. Am. B **28**, 171 (2011).

[35] J. Kasprzak, B. Patton, V. Savona, and W. Langbein, Nat. Phot. **5**, 57 (2011).

[36] See Section II.A of Supplemental Material at [URL] for description of the phase-referencing protocol.

[37] An example of the 2D FWM of GXB systems in the $\chi^{(3)}$ limit is provided in Fig. S6 of Supplemental Material at [URL].

[38] See Fig. S7 of Supplemental Material at [URL] for experimental results regarding the FWM imaging.

[39] See Section I of Supplemental Material at [URL] for theoretical details. A level scheme of the considered QD molecule, including all coupling-induced energy shifts, is shown in Fig. S1.

[40] See Fig. S7 of Supplemental Material at [URL] for experimental results regarding spectrally-resolved FWM amplitude retrieved from 2D FWM spectrum shown in Fig. 5 a.

[41] J. Kasprzak and W. Langbein, J. Opt. Soc. Am. B **29**, 1766 (2012).

[42] D. Abramavicius, B. Palmieri, D. V. Voronine, F. Sanda, and S. Mukamel, Chem. Rev. **109**, 2350 (2009).

[43] See Section I of Supplemental Material at [URL] for details regarding calculations of the FWM response.

[44] See Section I.C of Supplemental Material at [URL] for details regarding the model parameters.

[45] J. F. Specht, A. Knorr, and M. Richter, Phys. Rev. B **91**, 155313 (2015).

[46] See Section I.C and Fig. S3 of Supplemental Material at [URL] for theoretical simulations of the FWM spectra involving different origins of the coherent coupling.

[47] E. A. Stinaff, M. Scheibner, A. S. Bracker, I. V. Ponomarev, V. L. Korenev, M. E. Ware, M. F. Doty, T. L. Reinecke, and D. Gammon, Science **311**, 636 (2006).

[48] P.-L. Ardelt, K. Gawarecki, K. Müller, A. M. Waeber, A. Bechtold, K. Oberhofer, J. M. Daniels, F. Klotz, M. Bichler, T. Kuhn, H. J. Krenner, P. Machnikowski, and J. J. Finley, Phys. Rev. Lett. **116**, 077401 (2016).

[49] S. Kapfinger, T. Reichert, S. Lichtmannecker, K. Müller, J. J. Finley, A. Wixforth, M. Kaniber, and H. J. Krenner, Nat. Comm. **6**, 8540 (2015).

[50] F. Albert, K. Sivalertporn, J. Kasprzak, M. Strauß, C. Schneider, S. Höfling, M. Kamp, A. Forchel, S. Reitzenstein, E. A. Muljarov, and W. Langbein, Nat. Comm. **4**, 1747 (2013).

[51] E. W. Martin and S. T. Cundiff, arXiv:1705.04730v1 (2017).